Journal of Applied Physics

The effect of thermal annealing on the optical properties of Mg-doped zincblende GaN epilayers

Cite as: J. Appl. Phys. **130**, 085705 (2021); https://doi.org/10.1063/5.0057824
Submitted: 25 May 2021 . Accepted: 14 August 2021 . Published Online: 27 August 2021

D. Dyer, S. A. Church, M. Jain, M. J. Kappers, M. Frentrup, D. J. Wallis, R. A. Oliver, D. J. Binks, et al.

Journal of Applied Physics ARTICLE scitation.org/journal/jap

The effect of thermal annealing on the optical properties of Mg-doped zincblende GaN epilayers

Cite as: J. Appl. Phys. **130**, 085705 (2021); doi: 10.1063/5.0057824
Submitted: 25 May 2021 · Accepted: 14 August 2021 ·
Published Online: 27 August 2021

D. Dyer,[1] S. A. Church,[1] M. Jain,[2] M. J. Kappers,[3] M. Frentrup,[3] D. J. Wallis,[2,3,4] R. A. Oliver,[3] and D. J. Binks[1,a)]

AFFILIATIONS

[1]Department of Physics and Astronomy and Photon Science Institute, University of Manchester, Manchester M13 9PL, United Kingdom
[2]Kubos Semiconductors Ltd., Future Business Park, Cambridge CB4 2HY, United Kingdom
[3]Department of Materials Science and Metallurgy, University of Cambridge, Cambridge CB3 0FS, United Kingdom
[4]Centre for High Frequency Engineering, University of Cardiff, Cardiff CF24 3AA, United Kingdom

[a)]**Author to whom correspondence should be addressed:** david.binks@manchester.ac.uk

ABSTRACT

The effects of thermal annealing on the optical properties of Mg-doped cubic zincblende GaN epilayers grown by metalorganic chemical vapor deposition on 3C-SiC/Si (001) substrates are investigated. The photoluminescence spectra show near band edge features and a blue luminescence band that depend on Mg concentration, temperature, and excitation power density. Annealing the sample in a N_2 atmosphere causes the intensity of the blue band to increase by a factor of 5. Power dependent photoluminescence measurements show a reduction in the laser excitation density required for saturation of the blue band after annealing, indicating an increase in the recombination lifetime. Time decay measurements confirm this increase, which is attributed to a reduction in the concentration of non-radiative defects after annealing. The results presented here are compared to those reported previously for Mg-doped hexagonal wurtzite GaN.

INTRODUCTION

Light-emitting diodes (LEDs) based on InGaN/GaN quantum wells (QWs) grown in the wurtzite (wz) crystal phase emit light in the blue spectral region with an external quantum efficiency (EQE) > 80% and are used in combination with a yellow phosphor as the basis of efficient LED lighting.[1,2] However, producing white light by combining separate red, green, and blue LEDs would avoid Stokes' loss inherent to the use of the phosphor and also enable more control over the emitted spectrum of the lighting. While efficient red-emitting LEDs based on III-phosphide materials are available, intrinsic green-emitting devices with sufficient efficiency have not yet been produced—an issue which has become known as the "*green-gap*."[2,3] Green emission can be obtained from InGaN/GaN QWs by increasing the indium fraction but these devices have significantly reduced efficiency compared to their blue-emitting counterparts, having EQE's of typically 20%–50%[1] depending on the specific emission wavelength. There have been several mechanisms suggested for this reduction in efficiency.[1,3,4] The higher indium content needed to get into the green spectral region increases the polarization fields across the QW, which reduces the electron–hole overlap and, thus, the rate of radiative recombination. Also, the higher indium content is achieved by growing the QW at a lower temperature, resulting in a higher concentration of point defects that act as centers of non-radiative recombination.[4] Thus, overall, non-radiative recombination competes more successfully with radiative recombination in green wz QWs than their blue counterparts.

The zincblende (zb) crystal structure is an alternative GaN phase, which does not produce polarization fields across the QW, and the consequent reduction in radiative rate, when grown along the [001] direction.[5] It also has a smaller bandgap than wz-GaN[6] so that a smaller indium fraction is required to achieve green emission, despite the absence of the quantum confined Stark effect.[7] This allows higher InGaN growth temperatures to be used, thus decreasing the density of non-radiative recombination centers.

The p-type layer used in GaN-based LEDs is typically produced by doping with Mg, the effects of which have been investigated thoroughly for wz-GaN.[8–16] Passivation is a common problem in

metalorganic chemical vapor deposition (MOCVD) grown Mg-doped GaN and occurs when hydrogen introduced during growth forms electrically inactive complexes with Mg. These complexes must be dissociated for the material to be p-type,[9,16] which is typically achieved by post-growth thermal annealing.[9]

Reports of Mg-doped zb-GaN have so far been limited. Molecular beam epitaxy (MBE) grown layers have been studied on both GaAs and SiC/Si substrates and characterized by photoluminescence (PL) and Hall effect measurements.[17–22] The advantage of MBE grown Mg-doped GaN is that Mg-H complexes are less likely to form as there are no carrier gases used in this growth technique. However, MBE is not a scalable method for mass production of LEDs due to low growth rates and the long cycle times required to achieve an ultrahigh vacuum; in contrast, MOCVD is not limited by these factors. There has only been one report discussing the effects of annealing on MOCVD grown Mg-doped zb-GaN.[17] In this paper, the effects of pulsed laser annealing on its own and in combination with rapid thermal annealing on the room temperature optical properties of Mg-doped zb-GaN were studied.[17]

In this work, we investigate the effect of conventional thermal annealing in a N_2 atmosphere on the optical properties of Mg-doped zb-GaN epilayers grown by MOCVD on 3C-SiC/Si substrates. First, the Mg concentration, temperature, and excitation power dependence of the PL spectra are used to identify the features associated with Mg doping. The effect of annealing on the features is then studied using steady-state and time-resolved PL measurements.

EXPERIMENTAL METHOD

The GaN epilayers were grown by MOCVD in a 6×2-in. Thomas Swan close-coupled showerhead reactor on $2 \times 2\,cm^2$ pieces of a 150 mm diameter (001) 3C-SiC/Si substrate provided by Anvil Semiconductors Ltd. The substrate consists of a 2.7 μm thick layer of 3C-SiC grown on a 1.00 mm thick Si wafer with 4° miscut toward the [110] in-plane direction. Note that the lattice mismatch between zb-GaN and 3C-SiC is 3.4%.[23] A GaN nucleation layer was first grown followed by ~300 nm GaN and ~400 nm thick GaN:Mg epilayers. The Ga, Mg, and N sources were trimethylgallium (TMG), bis-(cyclopentadienyl)magnesium(II) (Cp_2Mg), and ammonia (NH_3), respectively, and hydrogen was used as the carrier gas, while nitrogen gas was used during the thermal annealing step. Further growth details can be found elsewhere.[24] The microstructure of samples grown by this method has previously been studied in detail,[25] where it was shown that stacking faults are the dominant defect, having a density of order $10^5\,cm^{-1}$. Moreover, these stacking faults can propagate to the surface, causing significant roughening.[26] Two sets of samples were grown. The first set consisted of a nominally undoped zb-GaN epilayer and two Mg-doped samples both annealed in N_2 atmosphere post-growth at a temperature of 740 °C for 1200 s. The Mg-doped samples were identical except for the Mg flow rate during growth, resulting in Mg concentrations of 8.6×10^{18} and $1.9 \times 10^{19}\,cm^{-3}$, as determined by secondary ion mass spectrometry (SIMS). The higher of these Mg concentrations is similar to that used in previous investigations of Mg-doped wz-GaN,[10,11] while the lower value results in PL spectra with more easily identifiable features, as will be seen below. The second sample set consisted of Mg-doped samples with the same concentration of $1.7 \times 10^{19}\,cm^{-3}$ but with only one sample thermally annealed (also in the reactor post-growth in a N_2 atmosphere at 740 °C for 1200 s). The Mg concentrations investigated here are similar to those investigated in Refs. 18 and 20 but lower by about an order of magnitude than the samples used in Ref. 17.

The SIMS analysis was performed commercially by Evans Analytical Group Laboratories and measured the concentration of Mg using a negative oxygen ion beam. X-ray diffraction (XRD) measurements were carried out using a PANalytical Empyrean diffractometer, equipped with Cu-Kα1 source, 2-bounce hybrid monochromator, and PIXcel solid state area detector. The optical properties of the samples were investigated using PL measurements to probe the carrier-dopant interactions. Steady-state PL measurements were obtained using a continuous wave (cw) HeCd laser emitting at 325 nm (3.8 eV) to excite the sample above the zb-GaN bandgap (3.3 eV at low temperature).[6] The sample temperature was controlled by attaching the samples onto the cold finger of a closed cycle He cryostat. The emission was collected by a spectrometer with resolution ≤5 nm and passed onto a cooled photomultiplier tube. The measured spectra were corrected for the system response using a calibrated black body source. Uniformity across a sample was checked by comparing spectra collected from different positions; and no significant difference in these spectra was observed, as shown in Fig. S1 in the supplementary material.

Time-resolved measurements were obtained using time correlated single photon counting (TCSPC) with pulsed excitation from a frequency tripled 80 MHz Ti-sapphire laser (wavelength 266 nm) to excite the samples above the zb-GaN bandgap. A cooled microchannel plate with a temporal resolution of 70 ps was used to detect the incoming single photons.

EXPERIMENTAL RESULTS

PL dependence on Mg concentration

The Mg concentration dependence of the 10 K PL spectrum is shown in Fig. 1, where all spectra have been normalized to the peak intensity. The undoped sample has three near band edge (NBE) peaks at 3.23, 3.11, and 3.05 eV, and there is also a broad band centered at ~2.9 eV. The spectral shifts of these features with both temperature and excitation power density, as shown in Figs. S3 and S4 of the supplementary material, respectively, allow the recombination processes associated with each to be identified. Thus, the peak at 3.23 eV is attributed to recombination of donor bound excitons (D^0X), while the 3.11 and 2.9 eV peaks are attributed to donor–acceptor pair recombination (DAP), and the 3.05 eV peak is attributed to recombination between an electron in the conduction band and a hole at the acceptor level (e, A^0), consistent with the previous work.[27] It has been reported elsewhere that the band around 2.9 eV is formed of two separate DAP peaks.[27] Therefore, the lower energy shoulder at 2.82 eV is attributed to a separate DAP recombination; the band as a whole is likely to be composed of a number of overlapping peaks corresponding to different types of donor and acceptor.

Figure 1 also shows that when zb-GaN is doped with Mg to $8.6 \times 10^{18}\,cm^{-3}$, the two DAP peaks at 2.82 and 2.9 eV are replaced by a broad blue emission band centered around 2.9 eV which

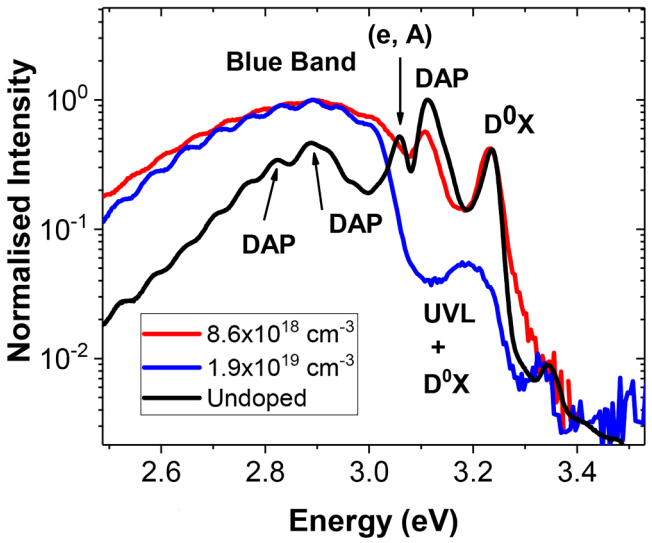

FIG. 1. Normalized 10 K PL comparison of nominally undoped and annealed Mg-doped zb-GaN samples. Samples were excited at a cw power density of 10 W cm^{-2}.

grows in intensity relative to the other spectral features. Increasing the Mg concentration further to 1.9×10^{19} cm^{-3} causes the relative intensity of the NBE emission to drop even more and is replaced by a weak and broad emission centered just below 3.2 eV. This feature likely results from the merging of the D^0X peak with a peak associated with Mg doping previously reported, which has been designated as the "ultraviolet luminescence" (UVL) band and attributed to either DAP recombination between a shallow donor and the Mg acceptor or (e, A^0) with Mg as the acceptor.[15,28,29]

The broad emission around 2.9 eV evident for zb-GaN after Mg doping has been reported previously and referred to as the "blue band."[18–20,22] The NBE peaks were also reported to disappear as the Mg concentration increases for MBE grown Mg-doped zb-GaN.[20] It has been previously suggested that the blue band emission in MBE grown Mg-doped zb-GaN was similar to that seen in Mg-doped wz-GaN[18] with the emission due to DAP recombination between a shallow Mg_{Ga} acceptor and V_N–Mg complex acting as a deep donor.[13] The peak shifts we observe for increasing temperature and excitation power density, as shown in the supplementary material, confirm that this is a feature associated with DAP recombination. The blue band peak position is similar for both the wz and zb crystal phases despite the change in the bandgap energy. This indicates that the change in bandgap energy is compensated by a change in another parameter associated with DAP recombination. Theoretical studies have suggested that the same donor in both crystal phases of GaN have similar ionization energies,[30,31] and Ref. 22 shows that the Mg ionization energy is again similar between the two crystal phases using both optical and electrical measurements.[22] This suggests a change in the average separation between donors and acceptors in the different crystal phases or another donor is responsible for the blue band recombination in Mg-doped zb-GaN. The temperature and power density dependent peak shifts of the 3.23 eV peak are consistent with D^0X recombination, as they were for the undoped sample—see the supplementary material. A weak peak at 3.35 eV, i.e., above the bandgap of zb-GaN, is present in the PL of all samples investigated and is attributed to small amounts of wz inclusions in the zb-GaN crystal matrix. However, the intensity of this emission is two orders of magnitude lower than the dominant recombination features in the spectrum, indicating wz inclusions have little effect on the optical properties of the samples.

Thermally annealed Mg-doped zb-GaN

Figure 2 compares the 10 K PL spectra of the annealed and unannealed Mg-doped zb-GaN epilayers. The blue band is the dominant feature in both spectra but NBE peaks are also evident and change after annealing. For the unannealed sample, the NBE is composed of a merged UVL band and D^0X peak with the latter evident as a high energy shoulder at 3.23 eV. There is also evidence of a small peak located above the bandgap of zb-GaN (3.3 eV) that is attributed to very small amounts of wz inclusions in the zb-GaN crystal matrix, in agreement with XRD measurements of the phase purity (see the supplementary material). The UVL band is significantly suppressed in the annealed spectrum obtained at 10 W cm^{-2}, and the D^0X peak is clearly defined again (however, as shown in Fig. S8 in the supplementary material, the UVL band is more evident at low power densities.) The suppression of the UVL band in Fig. 2 after thermal annealing suggests that it is associated with Mg–H complexes. The NBE PL spectrum of the annealed sample in Fig. 2 differs from that of the high Mg-doped sample shown in Fig. 1 when both are excited at 10 W cm^{-2} with the former retaining a distinct D^0X peak. However, the two spectra

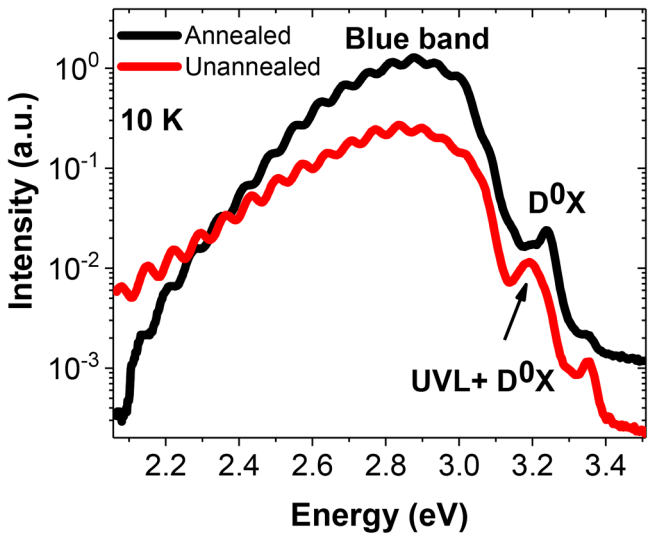

FIG. 2. 10 K PL comparison of Mg-doped zb-GaN samples with [Mg] = 1.7×10^{19} cm^{-3} before and after annealing in N_2. Samples were excited with a cw power density of 10 W cm^{-2}.

become similar as the excitation power density is reduced further (see Fig. S9 in the supplementary material), consisting in both cases of merged UVL and D^0X peaks, which illustrates the sensitivity of the NBE PL to the interplay between Mg concentration and excitation power density. Figure 2 also shows that the peak intensity of the blue band emission is increased significantly after annealing by a factor of ~5. Similar behavior has been observed in wz-GaN samples and attributed to the reduction in the density of Mg-H complexes by the annealing process.[9,15] Reference 17 reports an increase of the blue emission intensity (which itself is part of a broader emission feature) in the room temperature PL after pulsed laser annealing (PLA) of MOCVD grown Mg-doped zb-GaN,[17] which was attributed to the separation of Mg-H related complexes passivating the Mg-related deep donors. However, further rapid thermal annealing at 850 °C for 3 min of the same epilayers resulted in the reduction of the emission intensity,[17] in contrast to the increase in blue band emission obtained by the longer duration thermal annealing employed in our study. This behavior was attributed to the PLA not resulting in the removal of the dissociated H from the Mg-doped layer due to the short timescale of the laser pulses, thus allowing the Mg–H complexes to re-form during the subsequent rapid annealing stage.[17]

Figure 3 shows the spectrally integrated intensity of the blue band as a function of the excitation power density with the data fit with a straight line. The unannealed sample shows a linear relationship between intensity and excitation power density that does not change even at the highest power densities shown here. After annealing, in contrast, two distinct regions can be observed in the figure. For power densities up to 3.5 W cm^{-2}, there is a linear increase in intensity as power density increases similar to the unannealed sample. As the power density is increased above 3.5 W cm^{-2}, however, the intensity exhibits a sublinear relationship indicating that the blue band emission from the annealed sample is saturating. An increase in the density of optically active Mg acceptors following annealing might be expected to increase the saturation intensity of the blue band. However, since under cw excitation the steady-state carrier density increases with the recombination lifetime, a significant increase in this lifetime could increase the carrier density sufficiently to more than compensate for the increased acceptor density, resulting in the saturation behavior observed.

To investigate this further, low temperature time-resolved PL measurements were carried out on the annealed and unannealed samples, and the resulting decay transients are shown in Fig. 4. The decays consist of an initial fast component followed by a second slow component that, as shown in the inset, persists to the sub-millisecond time scale. Similar decays have been reported previously for Mg-doped wz-GaN.[32–34] It can be seen from Fig. 4 that the intensity of the blue band decays much more quickly prior to annealing, dropping to 1/e of the initial intensity in ~5.2 ns compared to ~21 ns after annealing. Similar behavior is seen for emission energies across the blue band as shown in Sec. S3 of the supplementary material in greater detail. The decays can be described by a combination of single and stretched exponential (as shown in Sec. S3 in the supplementary material). The stretched exponential, describing the long tail of the decay, is governed by the dispersion factor δ, which describes the level of disorder in the system.[35] The value of δ is in the range $0 < \delta < 1$, with $\delta = 1$ corresponding to complete order and $\delta = 0$ corresponding to complete disorder. As shown in S3 in the supplementary material, the value of δ increases upon annealing, suggesting a decrease in disorder. The different values of δ between the annealed and unannealed

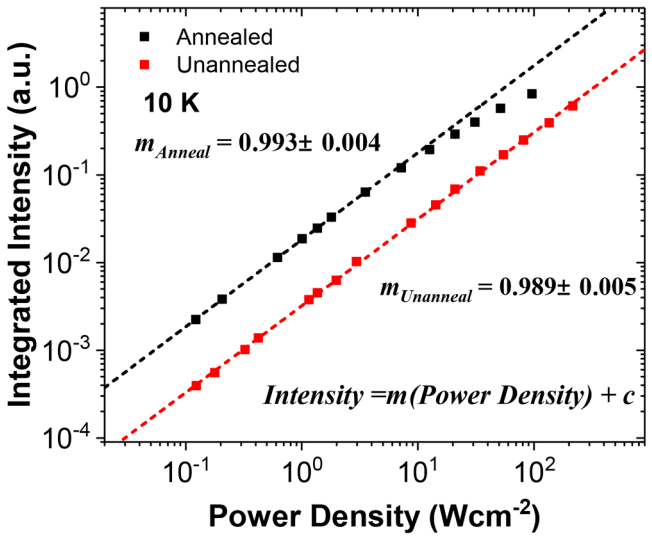

FIG. 3. Spectrally integrated intensity of the blue band emission as a function of the cw power density for both annealed and unannealed samples ([Mg] = 1.7 × 10^{19} cm^{-3}). The data points are fit with a straight line.

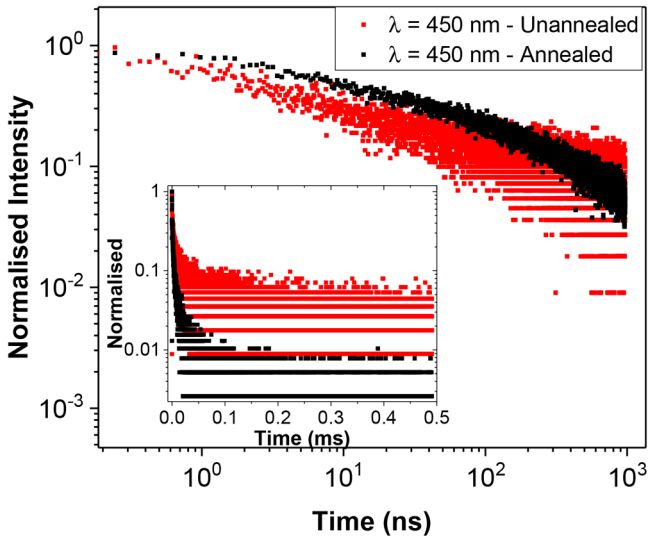

FIG. 4. PL decay transients for the annealed and unannealed Mg-doped zb-GaN samples ([Mg] = 1.7 × 10^{19} cm^{-3}) taken at a temperature of 10 K and at a wavelength of 450 nm, corresponding to the peak of the blue band emission in both samples. The inset shows the decays up to 0.5 ms.

samples result in the tails of the decays intersecting (at ~800 ns in Fig. 4) and the smaller δ value of the unannealed sample leads to its tail persisting to later times, as shown in the inset of Fig. 4.

The radiative lifetime of the blue band emission will decrease following annealing since the higher density of active Mg dopants (i.e., freed from the Mg–H complex) that this produces will decrease the average separation between the donors and acceptors. Since annealing produces an increase of the overall PL lifetime, then this suggests that there is a greater increase in the non-radiative lifetime associated with the blue band. A reduction in the non-radiative recombination in Mg implanted wz-GaN samples has also been reported following annealing based on photothermal deflection measurements[12] and attributed to the reduced density of V_N-V_{Ga} complexes after annealing. It should be noted that the samples investigated in Ref. 12 were annealed at temperatures in the range 1000–1300 °C for 5 min to recover the damage inflicted from ion implantation of the Mg.

XRD measurements (see the supplementary material) show that thermal annealing, under the conditions used in this paper, had no significant effect on the reciprocal space maps and intensity profiles along stacking fault streaks. Meaning both the phase purity and planar structural defects are unaffected by the annealing process. Thus, the decrease in non-radiative recombination is unlikely to be caused by planar defects such as stacking faults, which have been suggested to act as centers of non-radiative recombination in zb-GaN[36] and are the dominant defect in zb-GaN epilayers.[25] However, these XRD profiles do not provide information on lower dimensional defects such as threading dislocations (1D) and point defects (0D). Therefore, the dominant non-radiative recombination mechanisms in Mg-doped zb-GaN are likely associated with these.

CONCLUSION

In summary, the effect of thermal annealing on the optical properties of Mg-doped zb-GaN grown on 3C-SiC/Si (001) substrates by MOCVD has been investigated. A blue band was observed in the spectrum, which is associated with Mg doping. A significant increase in the intensity of this blue band (by a factor of 5) was observed when thermal annealing of the Mg-doped zb-GaN epilayers was carried out (at 740 °C in N_2 for 20 min), as previously observed for Mg-doped GaN in the wurtzite phase. Power density dependent measurements show that a lower saturation power density is observed for this emission band after annealing, and PL time decay measurements show that the recombination lifetime is significantly increased after annealing. It is, thus, concluded that thermal annealing both increases the density of active Mg dopants, thereby improving p-type conductivity, and decreases the density of non-radiative recombination centers in Mg-doped zb-GaN epilayers, in agreement with what is observed in Mg-doped wz-GaN.

SUPPLEMENTARY MATERIAL

See the supplementary material for XRD data, peak shifts with temperature and excitation power that identify spectral features of the samples, and further analysis of the blue band decay transients.

ACKNOWLEDGMENTS

The authors would like to acknowledge funding from the Engineering and Physics Sciences Research Council (EPSRC) for a studentship (Dyer) and for support under Grant Codes EP/R010250/1 and EP/R01146X/1. D. J. Wallis would like to acknowledge support through EPSRC fellowship No. EP/N01202X/2. The authors would also like to thank Dr. Peter Mitchell for helpful discussions on this work.

DATA AVAILABILITY

The data that support the findings of this study are openly available in the University of Manchester repository at http://doi.org/10.48420/14627817, Ref. 37.

REFERENCES

[1]M. Auf Der Maur, A. Pecchia, G. Penazzi, W. Rodrigues, and A. Di Carlo, Phys. Rev. Lett. **116**, 027401 (2016).
[2]M. H. Crawford, IEEE J. Sel. Top. Quantum Electron. **15**, 1028 (2009).
[3]B. Ding, Mater. Sci. Technol. **34**, 1615 (2018).
[4]S. Hammersley, M. J. Kappers, F. C. P. Massabuau, S.-L. Sahonta, P. Dawson, R. A. Oliver, and C. J. Humphreys, Phys. Status Solidi **13**, 209 (2016).
[5]D. J. As, Microelectron. J. **40**, 204 (2009).
[6]I. Vurgaftman and J. R. Meyer, J. Appl. Phys. **94**, 3675 (2003).
[7]D. R. Elsaesser, M. T. Durniak, A. S. Bross, and C. Wetzel, J. Appl. Phys. **122**, 115703 (2017).
[8]M. A. Reshchikov, P. Ghimire, and D. O. Demchenko, Phys. Rev. B **97**, 205204 (2018).
[9]S. Nakamura, N. Iwasa, M. Senoh, and T. Mukai, Jpn. J. Appl. Phys. **31**, 1258 (1992).
[10]A. Castiglia, J.-F. Carlin, and N. Grandjean, Appl. Phys. Lett. **98**, 213505 (2011).
[11]A. Klump, M. P. Hoffmann, F. Kaess, J. Tweedie, P. Reddy, R. Kirste, Z. Sitar, and R. Collazo, J. Appl. Phys. **127**, 045702 (2020).
[12]M. Sumiya, K. Fukuda, S. Takashima, S. Ueda, T. Onuma, T. Yamaguchi, T. Honda, and A. Uedono, J. Cryst. Growth **511**, 15 (2019).
[13]U. Kaufmann, M. Kunzer, M. Maier, H. Obloh, A. Ramakrishnan, B. Santic, and P. Schlotter, Appl. Phys. Lett. **72**, 1326 (1998).
[14]S. F. Chichibu, K. Shima, K. Kojima, S. Takashima, M. Edo, K. Ueno, S. Ishibashi, and A. Uedono, Appl. Phys. Lett. **112**, 211901 (2018).
[15]F. Shahedipour and B. W. Wessels, Appl. Phys. Lett. **76**, 3011 (2000).
[16]H. Amano, M. Kito, K. Hiramatsu, and I. Akasaki, Jpn. J. Appl. Phys. **28**, L2112 (1989).
[17]D. Xu, H. Yang, S. Li, D. Zhao, H. Ge, and R. Wu, J. Cryst. Growth **209**, 203 (2000).
[18]R. E. L. Powell, S. V. Novikov, C. T. Foxon, A. V. Akimov, and A. J. Kent, Phys. Status Solidi C **11**, 385 (2014).
[19]D. J. As, T. Simonsmeier, B. Schöttker, T. Frey, D. Schikora, W. Kriegseis, W. Burkhardt, and B. K. Meyer, Appl. Phys. Lett. **73**, 1835 (1998).
[20]E. Martinez-Guerrero, B. Daudin, G. Feuillet, H. Mariette, Y. Genuist, S. Fanget, A. Philippe, C. Dubois, C. Bru-Chevallier, G. Guillot, P. Aboughe Nze, T. Chassagne, Y. Monteil, H. Gamez-Cuatzin, and J. Tardy, Mater. Sci. Eng. B **82**, 59 (2001).
[21]D. Xu, H. Yang, D. G. Zhao, S. F. Li, and R. H. Wu, J. Appl. Phys. **87**, 2064 (2000).
[22]D. J. As, Phys. Status Solidi B **210**, 445 (1998).
[23]H. Okumura, K. Ohta, G. Feuillet, K. Balakrishnan, S. Chichibu, H. Hamaguchi, P. Hacke, and S. Yoshida, J. Cryst. Growth **178**, 113 (1997).
[24]L. Y. Lee, M. Frentrup, M. J. Kappers, R. A. Oliver, C. J. Humphreys, and D. J. Wallis, J. Appl. Phys. **124**, 105302 (2018).

[25]L. Y. Lee, M. Frentrup, P. Vacek, M. J. Kappers, D. J. Wallis, and R. A. Oliver, J. Appl. Phys. **125**, 105303 (2019).
[26]B. Ding, M. Frentrup, S. M. Fairclough, M. J. Kappers, M. Jain, A. Kovács, D. J. Wallis, and R. A. Oliver, J. Appl. Phys. **128**, 145703 (2020).
[27]D. Xu, H. Yang, J. B. Li, D. G. Zhao, S. F. Li, S. M. Zhuang, R. H. Wu, Y. Chen, and G. H. Li, Appl. Phys. Lett. **76**, 3025 (2000).
[28]M. A. Reshchikov and H. Morkoç, J. Appl. Phys. **97**, 061301 (2005).
[29]M. A. Reshchikov, J. Appl. Phys. **127**, 055701 (2020).
[30]F. Mireles and S. E. Ulloa, Appl. Phys. Lett. **74**, 248 (1999).
[31]H. Wang and A.-B. Chen, J. Appl. Phys. **87**, 7859 (2000).
[32]M. Godlewski, T. Suski, I. Grzegory, S. Porowski, J. Bergman, W. Chen, and B. Monemar, Phys. B Condens. Matter **273–274**, 39 (1999).
[33]Y.-H. Kwon, S. K. Shee, G. H. Gainer, G. H. Park, S. J. Hwang, and J. J. Song, Appl. Phys. Lett. **76**, 840 (2000).
[34]F. Shahedipour and B. W. Wessels, MRS Internet J. Nitride Semicond. Res. **6**, 12 (2001).
[35]S. A. Church, B. Ding, P. W. Mitchell, M. J. Kappers, M. Frentrup, G. Kusch, S. M. Fairclough, D. J. Wallis, R. A. Oliver, and D. J. Binks, Appl. Phys. Lett. **117**, 032103 (2020).
[36]R. M. Kemper, P. Veit, C. Mietze, A. Dempewolf, T. Wecker, F. Bertram, J. Christen, J. K. N. Lindner, and D. J. As, Phys. Status Solidi **12**, 469 (2015).
[37]D. Dyer, S. A. Church, M. Jain, M. J. Kappers, M. Frentrup, D. J. Wallis, R. A. Oliver, and D. J. Binks, "Dataset - the effect of thermal annealing on the optical properties of Mg-doped zincblende GaN epilayers," University of Manchester repository (2021).